J. Phys. Chem. A **2002,** *106,* 1081−1087

A High-Level Theoretical Study on the Gas-Phase Identity Methyl Transfer Reactions

Ikchoon Lee,*,[†] Chang Kon Kim,[†] Chang Kook Sohn,[‡] Hong Guang Li,[†] and Hai Whang Lee[†]

Department of Chemistry, Inha University, Inchon 402-751, Korea, and Department of Chemistry Education, Chonnam University, Kwangju 400-070, Korea.

Received: October 3, 2001; In Final Form: December 3, 2001

The gas-phase identity methyl transfer reactions, $X^- + CH_3X \rightleftharpoons XCH_3 + X^-$, have been investigated with X = H, F, Cl and Br at the MP2, B3LYP, QCISD and QCISD(T) levels by geometry and energy optimizations using the 6-311++G(3df,2p) basis sets at each level. Energy barriers, $\Delta E^{\ddagger}_{\mathrm{elec}}$, $\Delta E^{\ddagger}_{\mathrm{ZPE}}$, $\Delta H^{\ddagger}$ and $\Delta G^{\ddagger}$, are reported relative to both the reactants ($\Delta G^{\ddagger}$) and ion−dipole complex levels ($\Delta G^{\ddagger}_{\mathrm{c}}$). The electron correlation energy ($-E_{\mathrm{corr}}$) decreases in the MP2, QCISD and QCISD(T) results as the size (number of electron) of the system becomes larger (X = F → Cl → Br). The MP2 and QCISD methods underestimate the electron correlation effects relative to the highest level QCISD(T) results, which are, in general, in good agreement with the available experimental values. The lowest and highest activation barriers obtained with X = F and H, respectively, are found to be the consequences of the strong electrostatic interaction energies in the TS ($\Delta E_{\mathrm{es}} \ll 0$ and $\Delta E_{\mathrm{es}} \gg 0$, respectively), in contrast to small differences between nucleophiles, X, in the proximate $\sigma-\sigma^*$ charge transfer and deformation energies. The gas-phase barrier heights are in the order X = F < Br < Cl < H, and hence the reactivity and the gas-phase nucleophile strength are in the reverse order. Moreover, the extent of bond formation in the transition state, as expressed by the percentage bond order change, $\%\Delta n^{\ddagger}$, is also in the order of intrinsic nucleophilicity. Thus the stronger the nucleophile, the greater is the bond formation in the transition state for the intrinsic barrier controlled reactions.

Introduction

Bimolecular nucleophilic displacement (S_N2) reactions at carbon are one of the most important classes of reactions in organic chemistry. Methyl transfer reactions involving halides have long provided prototypes in this class, and in recent years the gas-phase methyl transfer reactions have come under close scrutiny both theoretically[1,2] and experimentally.[3] Of particular interest is the gas-phase identity chloride exchanges,

$$X^- + CH_3X \rightleftharpoons CH_3X + X^- \qquad (1)$$

X = Cl in eq 1, since the study of such reaction system is not only amenable to high-level theoretical methods due to its theoretically tractable small size, but also is feasible experimentally by monitoring the Cl^- isotopes. Despite the extensive works conducted to date, the gas-phase barrier height for the identity chloride exchange reaction of methyl chloride (X = Cl, eq 1) is still not certain. Experimental evidence of the barrier height comes from thermal rate measurements[3] but difficulty arises from the extremely short lifetime (<10 ps) of the ion−dipole complex (RC in Figure 1), $Cl^-\cdots CH_3Cl$,[3j] and recrossing of the barrier[2b] which leads to strong nonstatistical behavior in statistical modeling of the rate.[2] Theoretically the barrier height is sensitive to the level of accounting for electron correlation as well as to the size of basis set used in the calculations.[1] Thus experimental barrier height, $\Delta E^{\ddagger}$, reported for the chloride exchange ranges from 1.0 to 3.1 kcal mol^{-1} and theoretical correlated $\Delta E^{\ddagger}$ value varied from 1.8 to 3.2 kcal mol^{-1} (Table 1).

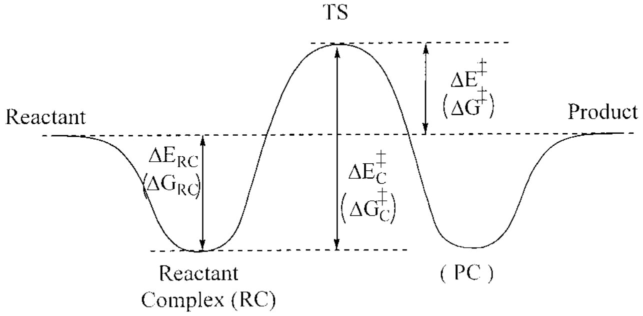

Figure 1. Double-well potential energy surface for the identity gas-phase methyl transfer reactions.

Ab initio results have been reported at various levels of theory on the identity methyl transfer reactions with chloride. However reports on the results with other anions, X = H, F and Br, are relatively scarce. Also the works on the identity methyl transfers with X = F, Cl and Br at a uniform level which is higher than the G2(+)(MP2) theory are scarce. Furthermore, high-level calculations reported are mostly limited to the potential energies, $\Delta E^{\ddagger}_{\mathrm{elec}}$. For comparison with the experimental results, however, the energies corrected for zero-point energy, $\Delta E^{\ddagger}_{(\mathrm{ZPE})}$, and for thermal energy (e.g., up to 300 K), $\Delta H^{\ddagger}$, are required, since the experimental barrier heights are based on thermal rate measurements and the energy lowering of up to 1.0 kcal mol^{-1} can be found for thermal corrections[2f] (vide infra). In addition entropy corrections ($-T\Delta S^{\ddagger}$) are also needed for free energy, $\Delta G^{\ddagger}$, calculation. Recently, Martin and co-workers[1k] reported extensive calculations on the gas-phase S_N2 reactions $Y^- + CH_3X \rightarrow CH_3Y + X^-$ (X, Y = F, Cl, Br) using their W1 and W2 ab initio computational thermochemistry methods. Their objective

---

* Corresponding author. Fax: +82-32-8654855. E-mail: ilee@inha.ac.kr.
[†] Inha University.
[‡] Chonnam University.

10.1021/jp013690h CCC: $22.00

TABLE 1: Selected Values of Barrier Height, $\Delta E^{\ddagger}$ (kcal mol^{-1}), Relative to Reactants for Reaction $Cl^- + CH_3Cl \rightleftharpoons CH_3Cl + Cl^-$ in the Gas Phase[a]

	$\Delta E^{\ddagger}$	method	ref
experimental	1 ± 1	RRKM	3b
	3.1	SCCVTST	2f
	2.5	RRKM/MCVTST	3f
	2.9 ± 0.2	PST	12
	<9.8	PST fit	3h
	$<10.8 \pm 3.6$	empirical threshold law fit	3h
ab initio	2.8	G2	3h
	2.7 (2.3)[b]	G2(+)	1h
	1.8	MP4	1f
	2.4	CBS-QB3	1k
	7.7	MP2/6-31++G**	1e
	7.4	CISD/DZDP	1d
	2.7 (3.0)[c]	CCSD(T)/367CGTOs	1j
	2.7	W2h	1k
	3.0 (2.5)[b]	QCISD(T)/6-311++G(3df,2p)	this work

[a] At 0 K. [b] Enthalpy of activation at 298 K. [c] The BSSE corrected value.

was solely to assess the quality of a number of calculation schemes such as G2, G3 and CBS-QB3 theories.

In this paper we report the results of high-level theoretical studies on the gas-phase methyl transfer reactions with X = H, F, Cl, Br in eq 1 at the QCISD(T) level of theory using the 6-311++G(3df,2p) basis sets. Both the level of electron correlation included and the basis sets used in the present work are higher than those of the G2(+) level,[4] since the G2(+) approximates calculations at the QCISD(T)/6-311+G(3df,2p) level.[5] The primary purpose of this work is to *examine factors that are responsible for the relative reactivity*, e.g., electron correlation effect in the TS, electrostatic and proximate charge transfer interaction etc.,[3] by *extending* the high-level methyl transfer studies to X = H, F, Cl and Br using a *uniform* theoretical level, QCISD(T)/6-311++G(3df,2p), and obtaining *four* clear-cut energetics, $\Delta E^{\ddagger}_{elec}$, $\Delta E^{\ddagger}_{(ZPE)}$, $\Delta H^{\ddagger}$ and $\Delta G^{\ddagger}$ (refer to computation section). We have compared the results at three lower levels, B3LYP, MP2 and QCISD with those at the QCISD(T) *using the same basis sets*, *6-311++G(3df,2p)*. In addition we have calculated up to free energies for the ion−dipole complexation, ΔG_{RC}, and the central energy barrier, $\Delta G^{\ddagger}_{c}$ (refer to Figure 1), at the same levels of theory throughout.

Computational Methods

Calculations were carried out using the Gaussian 98 set of programs.[6] Geometries of the reactants and stationary point structures were fully optimized at each level, B3LYP, MP2, QCISD and QCISD(T), using the 6-311++G(3df,2p) basis sets. All stationary points were characterized by harmonic vibrational analyses employing energy Hessians at two levels: MP2/6-311++G(3df,2p) and B3LYP/6-311++G(3df,2p). The stationary point energies (well-depth corresponding to the reactant complex, ΔE_{RC}, transition state energies with respect to reactants, $\Delta E^{\ddagger}$, and to the reactant complex, $\Delta E^{\ddagger}_{c}$) were evaluated at the B3LYP, MP2, QCISD and QCISD(T) levels using the 6-311++G(3df,2p) basis sets. These energies were then corrected for zero-point energies with application of appropriate scaling factors[7] (ΔE_{ZPE}) and for thermal energies (ΔH), and applied entropies to obtain free energies (ΔG) at 298 K. The natural bond orbital (NBO) analyses[8] were performed to estimate the proximate $\sigma-\sigma^*$ (including n−σ^*, n−π^*, $\sigma-\pi^*$, etc.) charge transfer energies in the reactants and transition states (TSs), and natural population analyses (NPA)[8a] were carried out. The percentage bond order changes at the TS ($\%\Delta n^{\ddagger}$)[9] were calculated by

$$\%\ \Delta n^{\ddagger} = \frac{n^{\ddagger} - n_R}{n_P - n_R} = \frac{[\exp(r^{\ddagger}/a) - \exp(r_R/a)]}{[\exp(r_P/a) - \exp(r_R/a)]} \times 100$$

where $r^{\ddagger}$, r_R and r_P are the bond length in the TS, reactant and product, respectively, and $a = 0.7$ was used. The bond orders, n_R, n_P and $n^{\ddagger}$, were defined by the Pauling relationship,[9a]

$$n_R = n_0, \quad n_P = n_0 \exp[(r_R - r_P)/a], \quad \text{and} \quad n^{\ddagger} = n_0 \exp[(r_R - r^{\ddagger})/a]$$

Since the reactions are identity exchanges, r_R of the C-LG (LG, leaving group) bond equals to r_P of the C−Nu (Nu, nucleophile) bond. However, in the $\%\Delta n^{\ddagger}$ values for the bond formation and bond cleavage, $r_R = \infty$ and $r_P = \infty$, respectively.

Results and Discussion

A. Reactants and Reactant Complexes. The gas-phase identity methyl transfer reactions proceed through a double-well potential energy profile, Figure 1. Initially, a reactant (ion−molecule) complex (RC) with C_{3v} symmetry is formed with a complexation energy of ΔE_{RC}. The RC then proceeds to the product complex (PC), which is identical to RC, through the transition state (TS) overcoming the central energy barrier ($\Delta E^{\ddagger}_{C}$). The activation energy with respect to the reactants is given as $\Delta E^{\ddagger}$. In the following, we differentiate and report four types of energy changes; namely, pure electronic energy (ΔE), zero-point-energy corrected potential energy at 0 K ($\Delta E_{(ZPE)}$), thermal energy corrected (to 298 K) value (ΔH), and the free energy ($\Delta G = \Delta H - T\Delta S$).

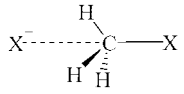

C_{3v}

Calculated geometries at the QCISD(T)/6-311++G(3df,2p) level for reactants (CH_3X) and RCs ($X^{\cdots}CH_3X$; C_{3v} structure) are listed in Table 2. Geometries optimized at lower levels (DFT, MP2 and QCISD) are summarized in S1 (Supporting Information). Other theoretical and experimental geometries available are also compared in Table 2. Our QCISD(T) [QCISD(T)/6-311++G(3df,2p)] geometries are in good agreement with the experimental values and are in better agreement than those at the G2+ (with MP2/6-311+G** geometries) and G2(+) (with MP2/6-31+G* geometries) levels.[1h] The C−X bond lengths are slightly stretched whereas those of C−H are slightly contracted in the RC relative to those in the respective reactant, except for X = H. These seem to arise from a weak charge transfer from X^- toward the σ^*_{C-X} LUMO ($n_X \rightarrow \sigma^*_{C-X}$) from the backside of the C−X bond in the RCs, which causes to weaken the C−X bond and strengthen the C−H bond to some extent.

The well-depths, ΔE_{RC}, corresponding to the ion−dipole complexation energies at the QCISD(T)/6-311++G(3df,2p) level, in Figure 1, are summarized in Table 3. The ΔE_{RC} values at the other lower levels (DFT, MP2 and QCISD) are summarized in **S2**.

Irrespective of the method of calculation used (DFT, MP2, QCISD or QCISD(T)) and of the level of energies expressed

TABLE 2: Geometries of Reactants and Reactant Complexes, with 6-311++G(3df,2p) Basis Sets (Bond Lengths in Å and Angles in Degrees)

species	level	r(C−X)	r(C⋯X)	r(C−H)	∠XCH
CH_3H	QCISD(T)	1.090		1.090	109.5
	expt[e]	[1.092]		[1.092]	[109.5]
		$(1.091)^d$		$(1.091)^a$	$(108.5)^a$
CH_3F	QCISD(T)	1.384		1.091	108.8
	expt[f]	[1.383]		[1.086]	[108.8]
		$(1.407)^a$		$(1.090)^a$	$(108.0)^a$
		$(1.405)^b$		$(1.087)^b$	$(108.2)^b$
CH_3Cl	QCISD(T)	1.784		1.087	108.5
	expt[g]	[1.776]		[1.085]	[108.6]
		$(1.780)^a$		$(1.089)^a$	$(108.9)^a$
		$(1.782)^c$		$(1.085)^c$	$(108.4)^c$
CH_3Br	QCISD(T)	1.946		1.086	107.9
	expt[h]	[1.934]		[1.082]	[107.7]
		$(1.954)^a$		$(1.088)^a$	$(108.0)^a$
$H^-\cdots CH_3H$	QCISD(T)	1.093	3.534	1.094	
		$(1.089)^a$	$(4.264)^a$	$(1.084)^a$	$(110.0)^a$
$F^-\cdots CH_3F$	QCISD(T)	1.431	2.569	1.084	108.7
		$(1.456)^a$	$(2.628)^a$	$(1.084)^a$	$(107.7)^a$
		$(1.453)^b$	$(2.609)^b$	$(1.080)^b$	$(107.8)^b$
$Cl^-\cdots CH_3Cl$	QCISD(T)	1.820	3.154	1.083	108.5
		$(1.810)^a$	$(3.270)^a$	$(1.085)^a$	$(108.8)^a$
$Br^-\cdots CH_3Br$	QCISD(T)	1.980	3.322	1.083	107.8
		$(1.988)^a$	$(3.395)^a$	$(1.084)^a$	$(107.8)^a$

[a] G2(+), ref 1h. [b] G2+, ref 1h. [c] CCSD(T)/367CGTOs, ref 1j. [d] MP2/6-31+G*, ref 1e. [e] Hehre, W. J.; Radom, L.; Schleyer, P. v. R.; Pople, J. A. *Ab Initio Molecular Orbital Theory*; Wiley: New York, 1986; Chapter 6. [f] Egawa, T.; Yamamoto, S.; Nakata, M.; Kuchitsu, K. *J. Mol. Struct.* **1987**, *156*, 213. [g] Jensen, T.; Brodersen, S.; Guelachrili, G. *J. Mol. Spectrosc.* **1981**, *88*, 378. [h] Graner, G. *J. Mol. Spectrosc.* **1981**, *90*, 394.

TABLE 3: Complexation Energies for the Identity Methyl Transfer $X^- + CH_3X \rightleftharpoons CH_3X + X^-$ at the QCISD(T)/6-311++G(3df,2p) Level (kcal mol^{-1}) (Experimental and Theoretical Results in Brackets and Parentheses)

R	ΔE_{RC}	ΔE_{RC}(ZPE)	ΔH_{RC}	$-T\Delta S_{RC}$	ΔG_{RC}
H	−2.87	−2.34	−2.73	3.27	0.5
		$(-0.5)^a$			
F	−14.62	−14.38	−14.58	5.47	−9.1
		$(-14.1)^b$	$(-13.6)^{c,o}$		
		$(-13.5)^d$	$(-13.7)^n$		
		$(-13.1)^d$			
		$(-13.1)^e$			
		$(-13.9)^a$			
Cl	−10.84	−10.63	−10.66	4.98	−5.7
		$(-10.6)^f$	$[-9.3 \pm 2.9]^g$	$[4.6 \pm 0.3]^h$	
		$(-10.5)^a$	$[-8.6 \pm 0.2]^h$	$(5.2)^k$	
		$(-10.6)^i$	$[-12.2 \pm 1.9]^l$		
		$(-8.8)^e$	$[-10.4]^j$		
		$(-10.8)^m$	$(-10.4)^c$		
		$(-9.7)^a$	$(-10.9)^n$		
Br	−10.02	−9.85	−9.81	5.52	−4.3
		$(-8.4)^e$	$[-11.2]^j$	$[6.6]^j$	
			$[-9.2]^h$		
			$(-10.0)^n$		

[a] 6-31++G**, ref 1e. [b] G2+, ref 1h. [c] G2(+), ref, 1h. [d] G2(+), ref 1i. [e] CISD(DZDP), ref 1d. [f] G2, ref 3h. [g] Collision induced dissociation, ref 3h. [h] NMR, ref 19. [i] MP4, ref 11. [j] HPMS, ref 3g. [k] MP4, ref 1f. [l] ICR, ref 10. [m] MP2/6-31G**, ref 2f. [n] Reference 1k. [o] Reference 1l.

TABLE 4: Some Calculated Values of Bond Length C−Cl in the TS ($r^{\ddagger}$, Å) and Barrier Heights, $\Delta E^{\ddagger}_{(ZPE)}$

method	$r^{\ddagger}$(C−Cl)	$\Delta E^{\ddagger}$(kcal mol^{-1})	ref
MP2/6-31+G*	2.315	4.6	1k
G2(+)	2.317	2.7 (2.3)[a]	1h
6-31G+MP4	2.382	3.6	2e
MP2/6-31G**	2.302	3.1	2f
CCSD(T)/367CGTOs	2.307	2.7	1j
MP2/6-31++G**	2.316	1.8	1f
QCISD(T)/6-311++G(3df,2p)	2.321	3.0	this work
B3LYP/6-311++G(3df,2p)	2.355	−1.1	this work
MP2/6-311++G(3df,2p)	2.286	4.8	this work
QCISD/6-311++G(3df,2p)	2.324	5.0	this work

[a] At 298 K.

(ΔE, $\Delta E_{(ZPE)}$, ΔH or ΔG), the well becomes deeper as the electronegativity of X increases, H < Br < Cl < F. This is a consequence of the stronger polarization, $C^{\delta+}-X^{\delta-}$, with the stronger electronegativity of X, which renders a stronger electrostatic complex with a more stable bond, $X^-\cdots C^{\delta+}$, due to an increased fractional ionic character of the bond. Since the ion−dipole complexes are weakly bound electrostatically, the complexation energies are not much dependent on the level of electron correlation that is accounted for and are similar irrespective of the method of calculation used (with the same basis set, 6-311++G(3df,2p)). Our results at the QCISD(T) level are in general in good agreement with the experimental values. Our result of ΔH_{RC} (−10.7 kcal mol^{-1}) for X = Cl is in excellent agreement with the recent experimental result of McMahon and co-workers (−10.4 kcal mol^{-1}).[3g,10] Noteworthy comparisons with those of other theoretical reports are the MP2/TZ3P+R+(2f,d) calculations extrapolated to MP∞ for X = Cl, −10.6 kcal mol^{-1},[11] and W2h result of Martin and co-workers of −10.9 kcal mol^{-1} [1k] for X = Cl, which are almost identical to our result. The G2+ level[12] ΔE_{ZPE} value (−14.1 kcal mol^{-1}) for X = F[1h] is in better agreement with our (higher level) value (−14.4 kcal mol^{-1}) than that at somewhat lower G2(+) level (−13.5 kcal mol^{-1}).[1h]

B. Transition Structures and Activation Energies. All the transition structures have D_{3h} symmetry with a trigonal bipyramidal pentacoordinate structure (TBP-5C). The TS geometries determined using the 6-311++G(3df,2p) basis sets at the HF, B3LYP, MP2, QCISD and QCISD(T) levels are summarized in S1. Both classical trajectory and quantum scattering calculations for the reaction with X = Cl have shown that the length of the C−Cl bond at the TS has a particularly strong effect on the reaction probabilities.[2c,g,h] Some calculated values of the C−Cl bond length $r^{\ddagger}$ (Å) at the TS together with the activation barriers are shown in Table 4. The C−X distances in the TS at the QCISD(T)/6-311++G(3df,2p) level for X = H, F, Cl and Br are $r^{\ddagger}$ = 1.646, 1.825, 2.321 and 2.479 Å respectively. We note that $r^{\ddagger}$ increases in the sequence, X = H < F < Cl < Br, which is also the sequence for the C−X distance in the reactants, H_3C-X (Table 2). However, the sequence of percentage bond-order changes, $\%\Delta n^{\ddagger}$, in the TS (which is a measure of the extent of bond formation in the TS) is H (39.6%) < Cl (40.9) < Br (41.1) < F (48.0). This order of the increasing extent of bond formation in the TS is exactly in the reverse order of the activation barriers, $\Delta G^{\ddagger}$, F ($\Delta G^{\ddagger}$ = 6.0 kcal mol^{-1}) < Br (8.5) < Cl (10.3) < H (52.4). Since according to the Marcus equation, eq 2, $\Delta G^{\ddagger}$ is an intrinsic barrier, $\Delta G^{\ddagger} = \Delta G^{\ddagger}_{o}$ (for $\Delta G^{\circ} = 0$), this indicates that the gas-phase intrinsic nucleophile strength of the anions increases in the order H < Cl < Br < F. Thus in an intrinsic-controlled reaction series, a

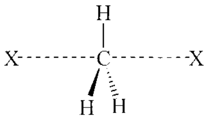

D_{3h} (TBP-5C)

stronger nucleophile leads to a greater degree of bond formation in the TS.

$$\Delta G^{\ddagger} = \Delta G^{\ddagger}_{o} + \frac{1}{2}\Delta G^{\circ} + \frac{(\Delta G^{\circ})^{2}}{16\Delta G^{\ddagger}_{o}} \tag{2}$$

The inverse proportionality between $\Delta G^{\ddagger}_{o}$ and $\%\Delta n^{\ddagger}$ could be applied, since the first derivative of the activation barrier ($\Delta G^{\ddagger}$) with respect to thermodynamic barrier (ΔG°) in the Marcus equation gives the expression for the degree of bond formation (β) as eq 3, where β is the Brönsted coefficient, and *in general* the degree of bond formation (β) is dependent on both the ΔG° and $\Delta G^{\ddagger}_{o}$ values.

$$\frac{\partial \Delta G^{\ddagger}}{\partial \Delta G^{\circ}} = \beta = \frac{1}{2} + \frac{\Delta G^{\circ}}{8\Delta G^{\ddagger}_{o}} \tag{3}$$

The gas-phase identity chloride exchange reaction, $Cl^- + CH_3Cl \rightarrow ClCH_3 + Cl^-$, is one of the most thoroughly investigated, both experimentally and theoretically, S_N2 reactions in organic chemistry.[1−3] Experimental evidence of the barrier height for the exchange reaction comes from thermal rate measurements,[3] which are within the experimentally observable range using the isotopes, ^{35}Cl and ^{37}Cl. Various experimental techniques are used in the rate measurement[3] such as ion cyclotron resonance (ICR),[3a,e,f,i] flowing afterglow-selected ion flow tube (FA-SIFT),[3c,d] SIFT/drift tube,[3b] high-pressure mass spectrometry (HPMS),[3g] guided ion beam tandem mass spectrometry[3h] (GIBMS), etc. The barrier height is then estimated by modeling of the energy dependence of the rate coefficient using statistical models such as RRKM theory,[3a,b,e,f,i] semiclassical canonical (SCCVTST)[2f] and microcanonical variational transition state theories[3f] (MCVTST) and phase space theory[13] (PST). The results of these experimental barrier heights, $\Delta E^{\ddagger}$, ranges from 1 ± 1 to 3.1 kcal mol^{-1} depending on the statistical modeling used as summarized in Table 1. The present result of $\Delta E^{\ddagger} = 3.0$ kcal mol^{-1} is in good agreement with experiment. For the identity chloride exchange reaction, the effects of different modes of energy on the dynamics have been examined by classical trajectories,[2a−c] semiclassical reaction path dynamics,[2d] and quantum scattering analyses on the multidimensional analytical potential energy surfaces (PESs) based on fits to ab initio calculations.[2e−h] Trajectory calculations of Hase and co-workers[2a−d] have shown that the reactant complexes (RC) have very short lifetimes (<10 ps) so that energy transfer between vibrational modes of RC and internal vibrational modes of CH_3Cl, which is required for reaction to occur, is very poor.[2h,3j] Due to this poor mode coupling, the reaction exhibits nonstatistical and non-RRKM effects, and places statistical modeling of the rate for estimating the reaction barrier in some doubt. The transition state theory has been also shown to break down due to significant recrossing of trajectories in the transition structure region[2b] and direct substitution without intermediate trapping in the potential well allowed by initial excitation of the reactant C−Cl vibration.[2a,d,e] These studies, therefore, question the validity of statistical theories for predicting and explaining the experimental measurements.

The barrier heights are calculated at various levels of theory for the low energy reaction path (backside attack S_N2 path) only (i.e., we have not considered the high energy frontside attack path)[3h] as listed in Table 1. The barrier height is sensitive to the level of electron correlation included and the size of basis set used. The highest level of theory used on the calculation of $\Delta E^{\ddagger}$ for the chloride exchange reaction is that by Botschwina,[1j] who has done coupled-cluster computations at the CCSD(T) level with basis sets up to 422 contracted GTOs (CGTOs). The results of this study show that the barrier height, $\Delta E^{\ddagger}_{(ZPE)}$, fluctuates and does not converge to a limiting value monotonically as the basis sets are increased from 2.2 kcal mol^{-1} (302 CGTOs) to 2.7 (367 CGTOs) to 2.5 (377 CGTOs) to 2.4 (421 CGTOs) and to 2.6 (422 CGTOs). The counterpoise correction for the basis set superposition error (BSSE) is found to raise the $\Delta E^{\ddagger}_{(ZPE)}$ values by 0.3 to ~0.5 kcal mol^{-1}. Thus the BSSE corrected value with 367 CGTOs is 3.0 kcal mol^{-1}. Our result of $\Delta E^{\ddagger}_{(ZPE)} = 3.0$ kcal mol^{-1} at the QCISD(T)/6-311++G(3df,2p) level is in close agreement with his recommended value of 2.7 ± 0.2 kcal mol^{-1}, which is also the W2h value of Martin and co-workers.[1k] We have made no attempt to correct for BSSE in view of the lack of agreement about the validity of such corrections.[14] For TSs, doing no BSSE correction is known to be better than any available counterpoise (CP) method.[15]

TABLE 5: Activation Energies (kcal mol^{-1}) for Reaction $X^- + CH_3X \rightleftharpoons CH_3X + X^-$ Calculated at the Various Levels with the 6-311++G(3df,2p) Basis Sets (* = Experimental and Theoretical Literature Values in Table 1; Experimental and Theoretical Results in Brackets and Parentheses)

method	X	$\Delta E^{\ddagger}$	$\Delta E^{\ddagger}_{ZPE}$	$\Delta H^{\ddagger}$	$-T\Delta S^{\ddagger}$	$\Delta G^{\ddagger}$
RHF	H	62.44	61.19	59.85	6.58	66.4
	F	7.71	7.64	6.83	8.19	15.0
	Cl	7.23	6.90	6.44	7.58	14.0
	Br	5.47	5.11	4.77	7.44	12.2
DFT	H	45.44	44.02	42.71	6.58	49.3
	F	−4.10	−4.34	−5.10	8.11	3.0
	Cl	−0.75	−1.14	−1.59	7.58	6.0
	Br	−2.38	−2.82	−3.16	7.46	4.3
MP2	H	49.97	48.69	47.34	6.65	54.0
	F	0.13	0.03	−0.80	8.27	7.5
	Cl	5.05	4.75	4.24	7.77	12.0
	Br	3.48	3.13	2.74	7.66	10.4
QCISD	H	50.92	49.64	48.29	6.65	54.9
	F	0.75	0.64	−0.19	8.27	8.1
	Cl	5.37	5.08	4.56	7.77	12.3
	Br	3.50	3.15	2.75	7.66	10.4
QCISD(T)	H	48.33	47.05	45.70	6.65	52.4
		(56.8)[a]	(56.4)[b]			
	F	−1.34	−1.45	−2.28	8.27	6.0
		(−1.1)[c]	(−1.4)[d]	(−1.7)[e]		
			(−2.5)[f]	(−2.6)[e]		
			(−1.8)[e]	(−0.9)[j]		
			(2.2)[g]	(−0.3)[k]		
			(−1.0)[h]			
	Cl*	3.31	3.01	2.50	7.77	10.3
	Br	1.57	1.22	0.82	7.66	8.5
			[1.3][i]	[1.3][i]		
			(2.5)[g]	(1.1)[e]		
			(1.4)[e]	(0.77)[k]		

[a] 6-31+G*, ref 1c. [b] CEPA, ref 1b. [c] MP2/6-31+G*, ref 1g. [d] G2(+), ref 1i. [e] G2(+), ref 1h. [f] MP4, ref 1f. [g] CISD(DZDP), ref 1d. [h] 6-31++G**, ref 1e. [i] RRKM(MCVTST), ref 3f. [j] Reference 1l. [k] Reference 1k.

Another interesting case is the barrier height at the MP4 level by Deng et al.[1f] (1.8 kcal mol^{-1}), which is somewhat lower than the accepted range of values (2.5−3.1 kcal mol^{-1})[3h] for the chloride exchange reaction. This is an example of the oscillating behavior of results obtained with the MP method around the limiting value.[16] It is often observed that MP4 overestimates the effect of the singles and triples contributions, since they enter the series for the first time at fourth order.[16]

The results with 6-311++G(3df,2p) basis sets summarized in Table 5 indicate that both the MP2 and QCISD underestimate the electron correlation effect. This is clearly indicated by electron correlation energies shown in Table 6, where we note

TABLE 6: Electron Correlation Energies (E_{corr})[a] Relative to RHF Level

		E_{corr} (au)				
	method	R	RC	TS	$\Delta E^{\ddagger}_{\mathrm{corr}}$ [b]	$\Delta E^{\ddagger}_{\mathrm{C,corr}}$ [c]
H	MP2	−0.21598	−0.21847	−0.23586	−12.47	−10.91
		(−0.21601)	(−0.21941)	(−0.23780)	(−13.67)	(−11.54)
	QCISD	−0.24789	−0.24981	−0.26590	−11.30	−10.10
		(−0.24799)	(−0.25051)	(−0.26648)	(−11.60)	(−10.02)
	QCISD(T)	−0.25346	−0.25623	−0.27595	−14.11	−12.37
		(−0.25361)	(−0.25726)	(−0.27664)	(−14.45)	(−12.16)
F	MP2	−0.71873	−0.72128	−0.73080	−7.57	−5.97
		(−0.71927)	(−0.72193)	(−0.73133)	(−7.57)	(−5.90)
	QCISD	−0.73276	−0.73553	−0.74385	−6.96	−5.22
		(−0.73325)	(−0.73618)	(−0.74425)	(−6.90)	(−5.06)
	QCISD(T)	−0.75374	−0.75716	−0.76816	−9.05	−6.90
		(−0.75444)	(−0.02972)	(−0.76865)	(−8.92)	(−6.61)
Cl	MP2	−0.56747	−0.57032	−0.57094	−2.18	−0.39
		(−0.56761)	(−0.57119)	(−0.57328)	(−3.56)	(−1.31)
	QCISD	−0.61546	−0.61758	−0.61841	−1.85	−0.52
		(−0.61563)	(−0.61818)	(−0.61942)	(−2.38)	(−0.78)
	QCISD(T)	−0.63041	−0.64207	−0.64544	−9.43	−2.11
		(−0.63065)	(−0.64294)	(−0.64662)	(−10.02)	(−2.31)
Br	MP2	−0.51527	−0.51797	−0.51844	−1.99	−0.29
		(−0.51544)	(−0.51909)	(−0.52097)	(−3.47)	(−1.18)
	QCISD	−0.55945	−0.56136	−0.56260	−1.98	−0.78
		(−0.55963)	(−0.56208)	(−0.56363)	(−2.51)	(−0.97)
	QCISD(T)	−0.58035	−0.58303	−0.58657	−3.90	−2.22
		(−0.58359)	(−0.58394)	(−0.58768)	(−4.45)	(−2.35)

[a] $E_{\mathrm{corr}} = E$(correlated level) − E(RHF). Values in parentheses are correlation energies obtained by using the optimized geometries at correlated levels. [b] $\Delta E^{\ddagger}_{\mathrm{corr}} = E_{\mathrm{corr}}(\mathrm{TS}) - E_{\mathrm{corr}}(\mathrm{R})$, in kcal mol^{-1}. [c] $\Delta E^{\ddagger}_{\mathrm{C,corr}} = E_{\mathrm{corr}}(\mathrm{TS}) - E_{\mathrm{corr}}(\mathrm{RC})$, in kcal mol^{-1}.

that electron correlation energies calculated using the geometries and energies optimized with the 6-311++G(3df,2p) basis sets are smaller by MP2 and QCISD than those of QCISD(T). There is very little improvement for the QCISD relative to the MP2 method. Reference to Table 6 reveals that the electron correlation energy ($-E_{\mathrm{corr}}$) decreases with the size (number of electrons) of the system, e.g., for R by MP2, F (0.7187) > Cl (0.5675) > Br (0.5153), except for X = H by an obvious reason of much smaller number of electrons. Irrespective of the method used, electron correlation energy ($-E_{\mathrm{corr}}$) is greater for a more strongly bound state (TS) than for a loosely bound (RC) and/or separated state (R). We can therefore conclude that the activation energies, i.e., the energy differences between the TS and the reactants ($\Delta E^{\ddagger}$), calculated by the MP2 and QCISD methods are overestimated due to the underestimated electron correlation energies (less negative) in the TS. The increment of correlation energy on going from the reactants to the TS ($\Delta E^{\ddagger}{}_{\mathrm{corr}}$ by the QCISD(T) method in Table 5) decreases in the order X = H ≫ F ≥ Cl > Br. Although QCISD(T) calculation is nearly size consistent, but recovers less and less electron correlation as the systems grow larger.[16] This lack of rigorous size consistency could be a factor contributing to such an order.

We note that for all nucleophiles (X) the successive inclusion of vibrational energies, from $\Delta E^{\ddagger}$ to $\Delta E^{\ddagger}_{(\mathrm{ZPE})}$ and to $\Delta H^{\ddagger}$ (also including Δ(PV) term), lowers the barrier heights irrespective of the method used. The predicted ordering of the barrier heights $\Delta E^{\ddagger}$ is F < Br < Cl < H, which is not in the sequence of decreasing nucleophilicity and increasing leaving ability predicted by the lower level calculations,[1a] $\mathrm{H}^- \rightarrow \mathrm{F}^- \rightarrow \mathrm{Cl}^- \rightarrow \mathrm{Br}^-$. The fact that the barrier height for the identity methyl transfer with X = F is lower than with X = Cl was first predicted in 1976 by Keil et al.[1b] based on their CEPA results, and later the ordering of $\Delta E^{\ddagger}$ was correctly established by Vetter et al.[1d] as F < Br < Cl in 1990 through CISD calculations with the DZDP basis sets, albeit their reported values of $\Delta E^{\ddagger}$ were rather high with $\Delta E^{\ddagger}_{(\mathrm{ZPE})} = 2.2$, 2.5 and 7.2 kcal mol^{-1} for X = F, Br and Cl, respectively. These $\Delta E^{\ddagger}$ values have been improved later successively through higher level calculations: F (−1.0 kcal mol^{-1}) < Cl (7.7) < H (54.7) at the MP2/6-31++G**level,[1e] and F (−1.9 kcal mol^{-1}) < Br (1.4) < Cl (2.7) at the G2(+) level.[1h] In the latter case, for Br the effective core potential (ECP) is used in the G2(+) procedure. At the MP4 level[1f] however the order for X = Cl and Br is reversed to F (−2.5 kcal mol^{-1}) < Cl (1.8) < Br (2.3). This could be due to the different basis set used for X = Br (6-31G** for Br and TZ3P+R+(2f,d) for F and Cl) in their MP4 calculations.[1f] The W2h $\Delta H^{\ddagger}$ values of Martin and co-workers[1k] are F (−0.34 kcal mol^{-1}) < Br (0.77) < Cl (2.67), which are in good agreement with our $\Delta H^{\ddagger}$ values with exception of F. Our results show that the orders are the same, F < Br < Cl < H, irrespective of the method used (even at the MP2 level). We emphasize that our QCISD(T) $\Delta E^{\ddagger}_{(\mathrm{ZPE})}$ results of F (−1.5 kcal mol^{-1}) < Br (1.2) < Cl (3.0) < H (47.1) are obtained *with the basis sets 6-311++G(3df,2p) for all reactions uniformly in the energy as well as in the geometry optimizations*. We therefore think that our $\Delta E^{\ddagger}$ (and $\Delta G^{\ddagger}$) values for the nucleophiles studied in the present work can be regarded as one of the most reliable ones among those reported so far.

The main factor contributing to the lowest energy barrier with X = F and the highest barrier with X = H is the electrostatic stabilization energy ($\Delta E_{\mathrm{es}} \ll 0$ for X = F and $\Delta E_{\mathrm{es}} \gg 0$ for X = H) in the TS. The ΔE_{es} values are −319 (F), −71 (Cl), −11 (Br) and 290 kcal mol^{-1} (H). These results of course come from the large differences in the magnitude of positive charge on the central carbon and of negative charge on X in the TS as shown in **S3** (Table of charge densities at the AIM-QCISD/6-311++G(3df,2p) level).

The proximate $\sigma-\sigma^*$ (including $n-\pi^*$, $\sigma-\pi^*$, $n-\sigma^*$, etc.) charge transfer energies,[8,17] $\Delta E^{(2)}_{\sigma-\sigma^*}$ in **S4**, and deformation energies (ΔE_{def})[18] are not much different for different X's. The deformation energies (ΔE_{def}) that are required for the substrates, $\mathrm{CH_3X}$, to form the TS geometries decrease in the order X = H > F > Cl > Br, and the gain in the charge transfer stabilization energies ($-\delta\Delta E_{\mathrm{ct}}$) on going from the reactants to the TS are also in the same order. These energy orderings do not correspond neither to the percentage C−X bond extension[9] (%$\Delta n^{\ddagger}$ for C−X; 60.4% (H) > 59.1 (Cl) > 58.9 (Br) > 52.0 (F)) nor to that of the activation barriers, $\Delta E^{\ddagger}$, H > Cl > Br > F. So the ΔE_{def} and $-\delta\Delta E_{\mathrm{ct}}$ are not simply related to the TS geometries and energies.

In fact the deformation energies (ΔE_{def}) are related to the binding energy of the C−X bond which is required to stretch in the TS, C−F (108 kcal mol^{-1}) ≥ C−H (104) > C−Cl (84) > C−Br (71).[19] The reversal of the order between C−H and C−F can be explained by the greater stretching (more than 10%) required for the C−H bond than the C−F bond in the TS. Since $\delta\Delta \mathrm{E}_{\mathrm{ct}}$ is the difference in the proximate $\sigma-\sigma^*$ charge transfer energies, i.e., $\delta\Delta E_{\mathrm{ct}} = \Delta E_{\mathrm{ct}}(\mathrm{TS}) - \Delta E_{\mathrm{ct}}(\mathrm{R})$, the order is related approximately to the vertical electron affinities (−EA) of the C−X bonds which are C−H (8 eV) > C−F (6.1) > C−Cl (3.7) > C−Br (0.9).[20] This is reasonable since a major charge transfer involves an n_{X}-$\sigma^*{}_{\mathrm{C-X}}$ interaction in which a lone pair electron on the nucleophile, X^-, is transferred to the σ^* orbital of the C−X bond in the activation process.[17]

C. Central Energy Barriers ($\Delta E^{\ddagger}_{\mathrm{C}}$). The central energy barriers ($\Delta E^{\ddagger}_{\mathrm{C}}$) are the barrier heights relative to the reactant complexes, $\Delta E^{\ddagger}_{\mathrm{C}} = -(\Delta E_{\mathrm{RC}} + \Delta E^{\ddagger})$ in Table 7. Since the complexation energy (ΔE_{RC}) for X = F is large negative, the order for $\Delta E^{\ddagger}_{\mathrm{C}}$ is different from that for $\Delta E^{\ddagger}$, Br (11.6) < F

TABLE 7: Central Energy Barriers of the Methyl Transfer Reactions (kcal mol^{-1}) (Experimental and Theoretical Results in Brackets and Parentheses)

method	Nu = LG	$\Delta E^{\ddagger}_{C}$	$\Delta E^{\ddagger}_{ZPEC}$	$\Delta H^{\ddagger}_{C}$	$-T\Delta S^{\ddagger}_{C}$	$\Delta G^{\ddagger}_{C}$
RHF	H	63.58	61.85	60.72	4.01	64.7
	F	20.17	19.79	19.15	2.84	22.0
	Cl	16.27	15.71	15.22	2.99	18.2
	Br	13.80	13.27	12.82	3.07	15.9
DFT	H	47.99	46.05	45.17	3.15	48.3
	F	10.02	9.66	9.07	2.72	11.8
	Cl	9.06	8.57	8.09	2.87	11.0
	Br	6.73	6.24	5.80	2.81	8.6
MP2	H	52.67	50.85	49.89	3.38	53.3
	F	14.20	13.86	13.23	2.79	16.0
	Cl	15.88	15.37	14.88	2.79	17.7
	Br	13.50	12.99	12.55	2.15	14.7
QCISD	H	53.48	51.67	50.71	3.38	54.1
	F	14.95	14.61	13.98	2.79	16.8
	Cl	15.74	15.24	14.75	2.79	17.5
	Br	13.02	12.51	12.07	2.15	14.2
QCISD(T)	H	51.20	49.39	48.43	3.38	51.8
	F	13.28	12.93	12.31	2.79	15.1
			(11.7)[a]	[11.0][b,c]		
			(12.4)[b]	(13.4)[g]		
			(11.8)[b]	(12.8)[h]		
	Cl	14.15	13.64	13.15	2.79	16.0
				(12.8)[b]		
				[12.9][c]		
				[13.2 ± 2.0][d]		
				(12.4)[e]		
				(13.6)[g]		
	Br	11.58	11.07	10.63	2.15	12.8
			[11.2][f]	(10.8)[b,e,g]		

[a] G2(+), ref 1i. [b] G2(+), ref 1h. [c] ICR, ref 3i. [d] SIFT/Drift, ref 3b. [e] MP4, ref 1f. [f] ICR, ref 3k. [g] Reference 1k. [h] Reference 1l.

(13.3) < Cl (14.2) < H (51.2 kcal mol^{-1}). The reversed order for Br and F (Br < F) is the result of the larger ΔE_{RC} value for X = F. In the gas-phase reaction the initially formed ion−dipole complex (RC) proceeds to the product complex (PC), which is identical to RC, through the central reaction barrier ($\Delta E^{\ddagger}_{C}$) in a reaction with the double-well potential surface. Since the central barrier heights ($\Delta E^{\ddagger}_{C}$) involve also the TS energies, the accurate experimental determinations of $\Delta E^{\ddagger}_{C}$ values are also limited by the nonstatistical and nontransition-state theory behaviors discussed above. However, the equilibrium constant measurements for the formation of the RC based on thermodynamic method[3g,10,11,21] were relatively accurate and hence the well-depth determined seems reliable. Thus, agreements between the theoretical and experimental values are better for the complexation energies (Table 3) than for the barrier heights ($\Delta E^{\ddagger}$ and $\Delta E^{\ddagger}_{C}$ in Tables 1, 4 and 6).

Summary and Conclusions

The gas-phase identity methyl transfer reactions, $X^- + CH_3X \rightleftharpoons XCH_3 + X^-$, are investigated with X = H, F, Cl and Br at the B3LYP, MP2, QCISD and QCISD(T) levels using 6-311++G(3df,2p) basis sets in the geometry and energy optimizations. The effect of electron correlation on the complexation energies differs very little between different levels. However, electron correlation is overestimated in the DFT (B3LYP) while it is underestimated in the MP2 and QCISD estimation of the barrier heights. The major contribution to the low and high activation barriers with X = F and H, respectively, is strong electrostatic interaction energy in the transition states ($\Delta E_{es} \ll 0$ and $\gg 0$, respectively) in contrast to small differences between nucleophiles, X, in the $\sigma-\sigma^*$ proximate charge transfer ($\Delta E^{(2)}_{\sigma-\sigma^*}$) and deformation ($\Delta E_{def}$) energies. The barrier height increases in the order X = F < Br < Cl < H, which is the reverse order of the extent of bond formation in the TS. Thus, for an intrinsic barrier controlled reaction series a stronger nucleophile (with a lower activation barrier) leads to a greater degree of bond formation in the TS. The QCISD(T)/6-311+G(3df,2p) geometries and energies are in general in good agreement with experiment.

Acknowledgment. This work was supported by grant No. R01-1999-00047 from the basic research program of the Korea Science and Engineering foundation. We also thank Inha University for support of this work.

Supporting Information Available: Tables of geometries, complexation energies, charge densities, and deformation, electrostatic, and second-order charge transfer energies. This material is available free of charge via the Internet at http://pubs.acs.org.

References and Notes

(1) (a) Shaik, S. S.; Schlegel, H. B.; Wolfe, S. *Theoretical Aspects of Physical Organic Chemistry. The S_N2 Mechanism*; Wiley: New York, 1992. (b) Keil, F.; Ahlrichs, R. *J. Am. Chem. Soc.* **1976**, *98*, 4787. (c) Sini, G.; Shaik, S. S.; Lefour, J.-M.; Ohanessian, G.; Hiberty, P. C. *J. Phys. Chem.* **1989**, *93*, 5661. (d) Vetter, R.; Zülicke, L. *J. Am. Chem. Soc.* **1990**, *112*, 5136. (e) Shi, Z.; Boyd, R. J. *J. Am. Chem. Soc.* **1990**, *112*, 6789. (f) Deng, L.; Branchadell, V.; Ziegler, T. *J. Am. Chem. Soc.* **1994**, *116*, 10645. (g) Lee, I.; Kim, C. K.; Chung, D. S.; Lee, B.-S. *J. Org. Chem.* **1994**, *59*, 4490. (h) Glukhovtsev, M. N.; Pross, A.; Radom. L. *J. Am. Chem. Soc.* **1995**, *117*, 2024. (i) Uggerud, E. *J. Chem. Soc., Perkin Trans. 2* **1999**, 1459. (j) Botschwina, P. *Theor. Chem. Acc.* **1998**, *99*, 426. (k) Tucker, S.; Truhlar, D. G. *J. Phys. Chem.* **1989**, *93*, 8138. (k) Parthiban, S.; de Oliveira, G.; Martin, J. M. L. *J. Phys. Chem. A* **2001**, *105*, 895. (l) Wladkowski, B. D.; Allen, W. O.; Brauman, J. I. *J. Phys. Chem.* **1994**, *98*, 13532.

(2) (a) Vande Linde, S. R.; Hase, W. L. *J. Chem. Phys.* **1990**, *93*, 7962. (b) Cho, Y. J.; Vande Linde, S. R.; Zhu, L.; Hase, W. L. *J. Chem. Phys.* **1992**, *96*, 8275. (c) Hase, W. L.; Cho, Y. J. *J. Chem. Phys.* **1993**, *98*, 8626. (d) Li, G.; Hase, W. L. *J. Am. Chem. Soc.* **1999**, *121*, 7124. (e) Vande Linde, S. R.; Hase, W. L. *J. Phys. Chem.* **1990**, *94*, 2778. (f) Tucker, S. C.; Truhlar, D. G. *J. Am. Chem. Soc.* **1990**, *112*, 3338. (g) Clay, D. C.; Palma, J. *J. Chem. Phys.* **1997**, *106*, 575. (h) Hernandez, M. I.; Campos-Martinez, J.; Villarreal, P.; Schmatz, S.; Clary, D. C. *Phys. Chem. Chem. Phys.* **1999**, *1*, 1197.

(3) (a) Pellerite, M. J.; Brauman, J. I. *J. Am. Chem. Soc.* **1983**, *105*, 2672. (b) Barlow, S. E.; Van Doren, J. M.; Bierbaum, V. M. *J. Am. Chem. Soc.* **1988**, *110*, 7240. (c) Van Doren, J. M.; DePuy, C. H.; Bierbaum, V. M. *J. Phys. Chem.* **1989**, *93*, 1130. (d) DePuy, C. H.; Gronert, S.; Mullin, A.; Bierbaum, V. M. *J. Am. Chem. Soc.* **1990**, *112*, 8650. (e) Wilbur, J. L.; Wladkowski, B. D.; Brauman, J. I. *J. Am. Chem. Soc.* **1993**, *115*, 10823. (f) Wladkowski, B. D.; Brauman, J. I. *J. Phys. Chem.* **1993**, *97*, 13158. (g) Li, C.; Ross, P.; Szulejko, J. E.; McMahon, T. B. *J. Am. Chem. Soc.* **1996**, *118*, 9360. (h) De Turi, V. F.; Hintz, P. A.; Ervin, K. M. *J. Phys. Chem. A* **1997**, *101*, 5969. (i) Craig, S. L.; Brauman, J. I. *J. Am. Chem. Soc.* **1999**, *121*, 6690. (j) Tonner, D. S.; McMahon, T. B. *J. Am. Chem. Soc.* **2000**, *122*, 8783. (k) Pellerite, M. J.; Brauman, J. I. *J. Am. Chem. Soc.* **1980**, *102*, 5993.

(4) Foresman, J. B.; Frisch, Æ. *Exploring Chemistry with Electronic Structure Methods*, 2nd ed.; Gaussian, Inc.: Pittsburgh, PA, 1996; p 152.

(5) (a) Petersson, G. A.; Malick, D. K.; Wilson, W. G.; Ochterski, J. W.; Montgomery, J. A., Jr.; Frisch, M. J. *J. Chem. Phys.* **1998**, *109*, 10570. (b) Pople, J. A.; Head-Gordon, M.; Raghavachari, K. *J. Chem. Phys.* **1987**, *87*, 5968. (c) Curtiss, L. A.; Raghavachari, K.; Pople, J. A. *J. Chem. Phys.* **1995**, *103*, 4192.

(6) Frisch, M. J.; Trucks, G. W.; Schlegel, H. B.; Scuseria, G. E.; Robb, M. A.; Cheeseman, J. R.; Zakrzewski, V. G.; Montgomery, J. A., Jr.; Stratmann, R. E.; Burant, J. C.; Dapprich, S.; Millam, J. M.; Daniels, A. D.; Kudin, K. N.; Strain, M. C.; Farkas, O.; Tomasi, J.; Barone, V.; Cossi, M.; Cammi, R.; Mennucci, B.; Pomelli, C.; Adamo, C.; Clifford, S.; Ochterski, J.; Petersson, G. A.; Ayala, P. Y.; Cui, Q.; Morokuma, K.; Malick, D. K.; Rabuck, A. D.; Raghavachari, K.; Foresman, J. B.; Cioslowski, J.; Ortiz, J. V.; Stefanov, B. B.; Liu, G.; Liashenko, A.; Piskorz, P.; Komaromi, I.; Gomperts, R.; Martin, R. L.; Fox, D. J.; Keith, T.; Al-Laham, M. A.; Peng, C. Y.; Nanayakkara, A.; Gonzalez, C.; Challacombe, M.; Gill, P. M. W.; Johnson, B.; Chen, W.; Wong, M. W.; Andres, J. L.; Gonzalez, C.; Head-Gordon, M.; Replogle, E. S.; Pople, J. A. *Gaussian 98*, Revision A.6; Gaussian, Inc.: Pittsburgh, PA, 1998.

(7) Scott, A. P.; Radom, L. *J. Phys. Chem.* **1996**, *100*, 16502.

(8) (a) Reed, A. E.; Curtiss, L. A.; Weinhold, F. *Chem. Rev.* **1988**, *88*, 899. (b) Glendening, E. D.; Weinhold, F. *J. Comput. Chem.* **1998**, *19*, 593. (c) Glendening, E. D.; Badenhoop, J. K.; Weinhold, F. *J. Comput. Chem.* **1998**, *19*, 628.

(9) (a) Houk, K. N.; Gustafson, S. M.; Black, K. *J. Am. Chem. Soc.* **1992**, *114*, 8565. (b) Lee, I.; Kim, C. K.; Lee, B.-S. *J. Comput. Chem.* **1995**, *16*, 1045. (c) Lee, J. K.; Kim, C. K.; Lee, I. *J. Phys. Chem. A* **1997**, *101*, 2893.

(10) Larson, J. W.; McMahon, T. B. *J. Am. Chem. Soc.* **1985**, *107*, 766.

(11) Wladkowski, B. D.; Lim, K. F.; Allen, W. D.; Brauman, J. I. *J. Am. Chem. Soc.* **1992**, *114*, 9136.

(12) Gronert, S. *J. Am. Chem. Soc.* **1993**, *115*, 10258.

(13) Graul, S. T.; Bowers, M. T. *J. Am. Chem. Soc.* **1994**, *116*, 3875.

(14) (a) Davidson, E. R.; Chakravorty, S. J. *Chem. Phys. Lett.* **1994**, *217*, 48. (b) Bernasconi, C. F.; Wenzel, P. J. *J. Am. Chem. Soc.* **1996**, *118*, 10494. (c) Saunders, W. H., Jr. *J. Am. Chem. Soc.* **1994**, *116*, 5400. (d) Schwenke, D. W.; Truhlar, D. G. *J. Chem. Phys.* **1985**, *82*, 2418.

(15) Lendvay, G.; Mayer, I. *Chem. Phys. Lett.* **1998**, *297*, 365.

(16) (a) Jensen, F. *Introduction to Computational Chemistry*; Wiley: Chichester, 1999; Chapter 4. (b) Szabo, A.; Ostlund, N. S. *Modern Quantum Chemistry. Introduction to Advanced Electronic Structure Theory*; McGraw-Hill: New York, 1989; p 265.

(17) Epiotis, N. D.; Cherry, W. R.; Shaik, S.; Yates, R.; Bernardi, F. *Structural Theory of Organic Chemistry*; Springer-Verlag: Berlin, 1977; Part IV.

(18) Shaik, S. S.; Schlegel, H. B.; Wolfe, S. *Theoretical Aspects of Physical Organic Chemistry. The S_N2 Mechanism*; Wiley: New York, 1992; p 167.

(19) Shaik, S. S.; Schlegel, H. B.; Wolfe, S. *Theoretical Aspects of Physical Organic Chemistry. The S_N2 Mechanism*; Wiley: New York, 1992; p 189.

(20) Shaik, S. S.; Schlegel, H. B.; Wolfe, S. *Theoretical Aspects of Physical Organic Chemistry. The S_N2 Mechanism*; Wiley: New York, 1992; p 142.

(21) Dougherty, R. C.; Dalton, J.; Roberts, J. D. *Org. Mass. Spectrum.* **1977**, *8*, 77.